Tribology and Materials
Vol. 3, No. 1, 2024, pp. 24-34

ISSN 2812-9717
https://doi.org/10.46793/tribomat.2024.002

An investigative study on different magnetic ionic liquids to be used as a lubricant and sealant in a vacuum pump

Tim EVANS *, Robert PALGRAVE

University College London, London, UK
*Corresponding author: tim.evans.18@ucl.ac.uk

Keywords
ionic liquid
magnetism
tribology
materials science
XPS
friction

History
Received: 01-11-2023
Revised: 12-12-2023
Accepted: 20-12-2023

Abstract

The aim of this work is to explore the possibility of using a magnetic ionic liquid as both a lubricant and sealant in a vacuum pump. The current lubricant in use is due to become obsolete due to incoming legislation on fluorinated compounds. The long-term goal is to use a magnetic field to hold the novel lubricant in place to create a better seal and thus reduce pressure more effectively whilst also lubricating the necessary mechanical parts. This paper explores physical properties (contact angle, viscosity, coefficient of friction (COF) and magnetism) and chemical properties (thermal stability and chemical stability as deduced by X-ray photoelectron spectroscopy (XPS)) of three ionic liquids based on imidazolium cations with varying length of alkyl side chain and a tetrachloroferrate anion along with two control lubricants which are used currently in the field and based upon perfluoropolyether (PFPE). The work shows that the three magnetic ionic liquids possess a lower COF value than the two control lubricants when measured using a Bruker UMT TriboLab suggesting they may perform better in the real life vacuum pump. Upon analysis of the three ionic liquid samples after tribological testing using XPS, it was shown that the ionic liquid samples displayed minor differences in spectra suggesting good stability with no obvious decomposition or degradation of the sample.

1. Introduction

To reduce the cost of friction, wear and corrosion lubricants are used. Lubricants can be traced back as far as ancient Egyptian times when animal fats known as tallow were used to lubricate the axles of chariots [1]. It was not until the 1950s when the first synthetic lubricants were developed, primarily for the use of aviation and aerospace industries where the first large-scale commercially available synthetic oil came in 1972 [2].

The aim of this work is to explore a magnetic lubricant that can eventually act as both a lubricant and sealant in a vacuum pump [3]. The current lubricant in use is based on a type of perfluoropolyether (PFPE) which is a type of synthetic oil of which the actual structure is a trade secret which must be phased out due to incoming legislation. To achieve this, an ionic liquid (IL) is to be used. The use of ionic liquids as lubricants can be traced back to 2001 with the first original publication completed by Ye et al. [4]. Since this date, a plethora of work has amounted exploring ionic liquids as pure lubricants, additives in existing lubricants and hybrid materials [5-14]. Early breakthroughs regarding ILs in tribology noted that fluorinated anions such as BF_4^- could be hydrolysed in the presence of moisture to produce HF which then resulted in corrosion of the surfaces in use. However, some authors believe this corrosion can be beneficial to forming a tribofilm which reduces wear. The avoidance of fluorinated anions led to the works by Guo et al. [5] and González et al. [6] who explored anions based on carboxylates such as hexanoates and octanoates. It is described that these resulting ILs adsorb strongly on the steel surfaces and form a protective boundary film.

However, the study of ionic liquids can be traced even further back, often cited as 1914 when Paul Walden prepared ethylammonium nitrate [15], however from then until 1975 the field was relatively quiet until other authors such as Chum et al, Nanjundiah et al. and Wilkes et al. brought ionic liquids to the forefront of science [16-18]. An ionic liquid (IL) has many definitions, however, for the purpose of this work it can be defined as a liquid at room temperature, with room temperature being defined as between 17 and 23 °C as opposed to a substance that is a liquid below 100 °C which is sometimes quoted in the literature. An IL is made up purely of positively and negatively charged ions that *result* in a liquid, not to be confused with a salt dissolved in a carrier solvent which is not the same. They are often termed designer solvents, not because they are a highly-priced commodity but because their properties can be tailored to specific problems with the easiest example being a PF_6 anion will result in a hydrophobic IL and a BF_4 anion will result in a hydrophilic IL.

The work is based on magnetic ionic liquid (MIL) samples which demonstrate paramagnetism which is when a material becomes magnetised in a magnetic field but disappears when the field is removed. This is achieved through a paramagnetic anion, which was first achieved by Hayashi and Hamaguchi in 2004 [19]. Further, this is also not to be confused with a ferrofluid which is where magnetic nanoparticles are dispersed in a carrier solvent. Ferrofluids would not be a feasible solution to the problem as it is anticipated due to the high temperatures of the operating equipment it would be likely the carrier solvent would evaporate, as well as potential pollution to the vacuum from solid nanoparticles. Recent work carried out by Jia et al. [20] explores a dysprosium-based paramagnetic IL compared with a ferrofluid in relation to tribological studies. Again, the superior tribological properties of the IL are ascribed to the ability of the sample to form effective boundary films on the steel surface for which it was tested. This work proves that the use of an IL is far superior than using a ferrofluid which is described as having the nanoparticles accumulate on the surface causing abrasion.

The purpose of this work is to explore MILs as a potential replacement lubricant and sealant in vacuum equipment. This work aims to build on existing work by exploring iron-based anions and imidazolium-based cations as paramagnetic lubricants.

2. Experimental

All chemicals were used as bought from Sigma-Aldrich with no further purification techniques, with purity as stated. Methylimidazole 99 %, chlorobutane 99 %, chlorooctane 99 %, chlorodecane 98 %, iron(III) chloride hexahydrate 97 % and solvents including acetonitrile 99.5 % and deionised water, were used as acquired along with deuterated dimethyl sulfoxide and deuterated chloroform for nuclear magnetic resonance (NMR) experiments. Fomblin and Leybonol were kindly provided by Edwards Vacuum Ltd company and used as controls in the experiments based on perfluoropolyether composition.

^{1}H NMR and ^{13}C ^{1}H NMR were recorded at 500/400 MHz and 125/100 on Bruker Avance 500/400 spectrometers. All spectra are referenced to $(CD_3)_2SO$ residual solvent peaks (^{1}H NMR δ = 2.50 ppm; ^{13}C ^{1}H NMR δ = 39.52 ppm). All chemical shifts are quoted in parts per million (ppm), measured from the centre of the signal except in the case of multiplets which are quoted as a range. Coupling constants are quoted to the nearest 0.1 Hz. Splitting patterns are abbreviated as follows: broad singlet (br. s), singlet (s), doublet (d), triplet (t), quartet (q), quintet (quin), sextet (sext), multiplet (m) and combinations thereof. Raman spectra were acquired using a Renishaw inVia Raman microscope with a 50 × objective in a backscattering configuration. The excitation wavelength was 785 nm (130 mW, 10 %) and the acquisition time was 20 s. The laser spot size was around 1 μm^2.

Magnetic susceptibility was measured using a Sherwood Scientific magnetic susceptibility balance (MSB) mark 1 with a magnetic field strength of 3.5 kG. Magnetism measurements were completed by initially weighing 0.2 g of the sample and recording the weight of a magnetic susceptibility tube, as well as noting the calibration constant of the Evans balance to be used. The range knob was set to '× 1' and the zero knob was adjusted until the display read 000. The empty tube was inserted into the machine and the reading was taken (R_0). The empty tube was then filled with 0.2 g of the sample that was measured previously being careful to avoid spillages and then re-weighed. This filled tube was then placed into the balance and a new reading was taken (R). Once complete the length of the sample in the Evans tube was measured with a micrometer and then emptied. A new clean Evans tube was used for each measurement.

Thermogravimetric analysis (TGA) measurements were recorded on a TA Instruments TGA 5500.

Unless stated otherwise, measurements began at room temperature and ramped at 10 °C per minute up to 450 °C in air. Thermal stability measurements were taken by weighing 10 mg of specified sample and then heating from room temperature (the tests never began at higher than 30 °C) at a ramp rate of 10 °C per minute up to 450 °C in air.

Viscosities were measured using a Brookfield DV-III rheometer with an SC-27 spindle and an additional small sample adapter, with a water jacket and external water bath for temperature regulation. Viscosities were recorded once a stable value had been reached. Viscosity indexes were measured using a water bath with a built-in circulator, which was used to pump heated water through the water jacket built into the small sample adapter. Viscosities were measured from 30 to 80 °C in 10 °C steps. As stated in the results section the temperature was only able to reach 80 °C, where the internal temperature of the viscometer was displayed to ensure the correct temperature had been reached before measurements were taken.

For contact angle measurements, steel plate with *Ra* ~ 1.5 µm, aluminium 1.5 mm thick mill finish plate with *Ra* ~ 7.5 µm and 0.5 mm thick rubber sheet grade A vinylidene fluoride hexafluoropropylene, known by its brand name Viton with *Ra* ~ 0.8 µm, were used. Contact angles were measured using a Krüss DSA25E contact angle goniometer with a standard automated syringe dosing unit. Contact angles were measured by loading a syringe with the specified sample and dispensing 2 µl of each specified sample at a dispense rate of 0.05 µl/s onto different substrates. Each substrate, steel, aluminium and rubber sheet was cleaned with acetone and allowed to dry before being used. A video recording was then taken with a trigger point to start the measurement once the touch-on method had been used to acquire the droplet. Each measurement was taken 3 times. Data analysis of contact angles were completed using FTA32 video 2.1 software, where the baseline of the droplet was set in the software and measured using a non-spherical fit. The measurement published is a timed average as the droplet spreads.

Tests to measure the coefficient of friction (COF) were completed using a Bruker UMT TriboLab utilising a ball on a reciprocating plate test. A carbon steel plate of 5.5 × 4.2 cm with *Ra* ~ 1.5 µm, was coupled with a 10 mm diameter 52100 bearing steel ball with *Ra* ~ 0.1 µm. The independent variables under control were the duration of the test, normal load and reciprocating velocity. To produce COF curves, the load was set to a constant of 5 N, with reciprocating speeds increasing from 0.1 to 20 Hz in different steps, i.e. 0.1, 0.5, 1, 2, 4, 6, 8, 10, 12, 14, 16, 18 and 20 Hz. Each step lasted 180 seconds with a stroke length of 4 mm and data acquired at roughly every 0.02 seconds using roughly 2 ml of sample per test. All measurements were completed at room temperature, as there were no heating or cooling elements involved in data acquisition. Control tests were performed on Fomblin and Leybonol for COF curves. The COF values reported are timed averages at each step. The data was collected using a steel plate, which was cleaned with acetone between measurements along with a new steel ball every time. Only one run was completed for each sample.

The X-ray photoelectron spectra of all the samples were recorded using a K-Alpha spectrometer equipped with a monochromated, micro-focused, Al K-Alpha X-ray source (1486.6 eV). A quartz crystal monochromator set in a 250 mm Rowland circle, hybrid optics, multichannel plate, hemispherical analyser and 128-channel sensitive detector. Samples were prepared and 2 drops of each sample were placed onto a stainless steel plate and placed under vacuum. There were no significant bubbling and outgassing observed in this process. After achieving the required pressure, the samples were transported to the main analytic vacuum chamber for analysis. A 500 eV Ar+ ion dual beam flood gun was used to achieve the charge compensation.

3. Results and discussion

3.1 Ionic liquid samples investigated

The samples studied in this work were prepared following a procedure set out by Hayashi et al. in their seminal paper of 2004 [19]. In brief, methylimidazole was alkylated with a chlorinated alkane to create the intermediate structure which was confirmed with proton and carbon NMR. An anion exchange step was then completed using $FeCl_3 \cdot 6H_2O$ which was an endothermic reaction followed by drying under vacuum to give pure ionic liquid samples where the anion structure was confirmed with Raman spectroscopy where 1 peak was observed due to Fe–Cl bonds at roughly 333 cm^{-1}. The nomenclature used in this work follows the numbering system whereby the numbers in subscript refer to the length of the alkyl chain bonded to nitrogen in the imidazolium ring. The

samples can be seen in Table 1 along with a generic cation structure with the tetrachloroferrate anion in Figure 1. The controls in this work are named Fomblin and Leybonol, brand names and their composition are largely trade secrets with both based on a PFPE-type lubricant.

Table 1. Ionic liquid samples analysed

Sample	Cation	Anion
1	C_4C_1Im	$FeCl_4$
2	C_8C_1Im	$FeCl_4$
3	$C_{10}C_1Im$	$FeCl_4$

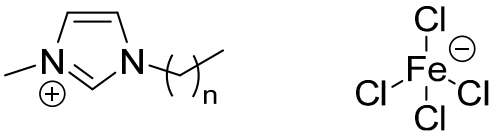

Figure 1. Methylimidazolium cation with varying alkyl component and iron-based anion

3.2 Magnetism

Magnetism is a key area to perform, where it is hoped that whilst working in the rotary vane pump the lubricant will be able to be held in place with an external magnet to create the seal to in turn allow the pump to reduce pressure. Paramagnetism was assessed using an Evans balance, applying the mass magnetic susceptibility Equation (1) presented below with results presented in Table 2.

$$\chi_g = \frac{L}{m}[C(R-R_0)]\cdot 10^{-9}, \quad (1)$$

where L is sample length in cm, m is sample mass in g, C is balance calibration constant (unique to each balance), R is the measurement taken when the sample is inside the tube and R_0 is the measurement taken when the tube contains no sample.

Equation (1) gives a value of χ_g in centimetre-gram-second (cgs) units of erg G^{-1} g^{-1}. This can then be converted into the molar susceptibility χ_m by multiplying by the relative molecular mass (RMM) of the corresponding sample.

$$\chi_m = \chi_g \cdot RMM. \quad (1)$$

This gives an χ_m value in units of erg G^{-1} mol^{-1} but can also be represented as cm^3 mol^{-1}. However, a correction must now be made as all compounds have pairs of electrons which will be weakly repelled from the magnetic field therefore meaning a diamagnetic correction must be made.

This is completed by adding up the diamagnetic contributions of all the atoms in the molecule by using a paper published by Bain and Berry [21] which contains the data. This then produces the following equation which is a correction:

$$\chi_{m_{corr}} = \chi_m - \chi_{m_{dia}}. \quad (3)$$

The final step is then to calculate the effective magnetic moment μ, using the Curie's law:

$$\mu = 2.84(\chi_{m_{corr}} T)^{0.5}, \quad (4)$$

where T is the temperature in K.

Once the effective magnetic moment has been calculated, this can then be put into the spin-only formula where it is assumed only spin contribution is contributing to the magnetic moment:

$$\mu = [n(n+2)]^{0.5}. \quad (5)$$

This equation reveals the number of unpaired electrons present in the sample and can be used as another method of confirming the structures that have been synthesised, for example, the iron-containing samples have iron in its +3 oxidation state, resulting in 5 unpaired electrons assuming they are in high spin configuration which is a reasonable assumption as halogens such as chlorine and bromine lead to high spin complexes; therefore meaning a value of 5 should be the output from the spin-only formula.

Table 2. Measured magnetic susceptibility, with expected values based on literature and their corresponding n values; adapted from Evans [3], licensed under CC BY-NC 4.0

Sample	Measured μ, erg G^{-1}	Expected μ, erg G^{-1}	n (calculated from spin-only formula)
1	5.70	5.92	5.61
2	5.94	5.92	5.02
3	5.74	5.92	4.82

As can be seen in Table 2, the magnetic moment has been calculated, and the expected value is 5.92 where the experimental values here vary between samples but this can be accredited to the difficulty in physically manipulating and preparing samples to be measured. Further to this, the spin-only formula can also be used as a method of confirming structure as the value of n should be 5 equating to 5 unpaired electrons (the reason for paramagnetism). Reasons for deviations from this value could be dilution resulting in a value lower than 5 which can be seen for sample 3; however, in general the results agree with those of the experimental literature [22].

3.3 Thermal stability

The vacuum pump the lubricant will operate in has an operating temperature of around 85 °C. To ascertain if the samples will be sufficiently stable at this temperature an accelerated test was performed. The sample was heated to 450 °C where decomposition temperatures can be seen in Figure 2.

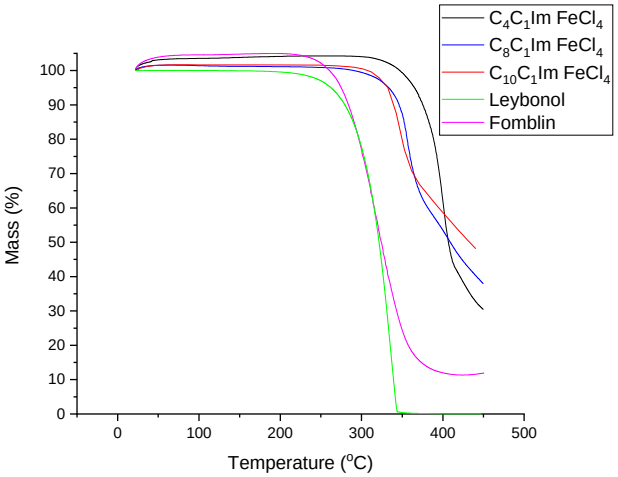

Figure 2. TGA graphs for all samples; adapted from Evans [3], licensed under CC BY-NC 4.0

From the graphs, it can be seen that all 3 MIL samples have a higher decomposition temperature than the two control lubricants, and all of the samples show no change in mass at 85 °C. The IL samples appear to begin decomposition close to 350 °C whereas the control samples appear to begin decomposition close to 300 °C.

3.4 Viscosity and viscosity index

The viscosity data for all tested samples are presented in Table 3.

Table 3. Room temperature dynamic viscosity measurements

Sample	Dynamic viscosity at 20 °C, mPas
1	46
2	84
3	150
Fomblin	463
Leybonol	258

We can see that lengthening the alkyl chain attached to the imidazolium cation affects the viscosity of the sample; increasing the alkyl chain appears to increase the viscosity. However, the 3 samples still have viscosities that are lower than the two control samples. To build on this, viscosity indexes were also calculated. It is anticipated that the upper operating temperature of the machinery that the lubricants will be used in is likely to be around 85 °C, therefore we have measured how the viscosity changes as the temperature is increased. The data can be seen in Figure 3.

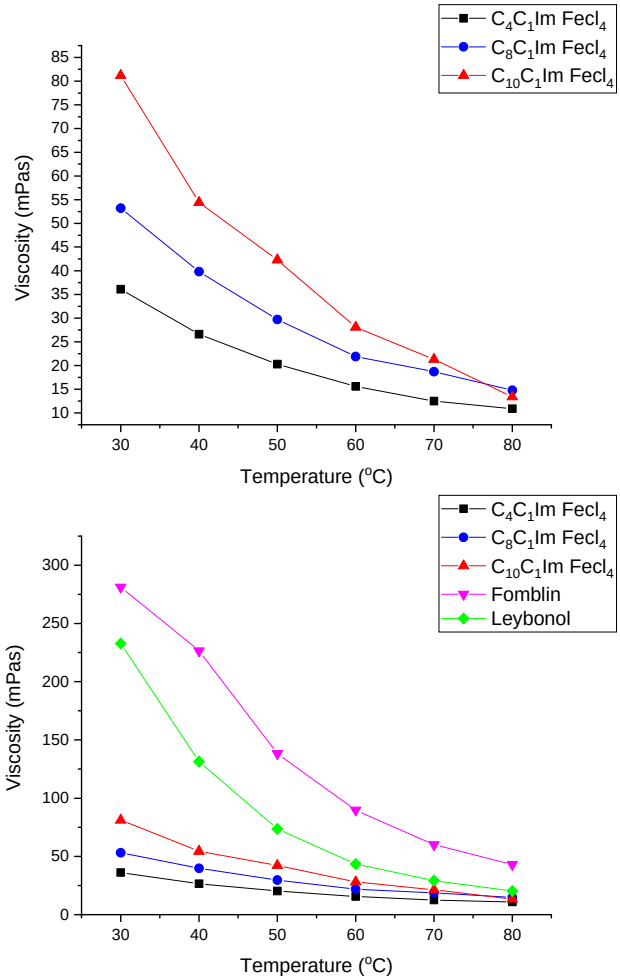

Figure 3. Viscosity vs. temperature graphs for all tested samples; adapted from Evans [3], licensed under CC BY-NC 4.0

From these graphs, the higher viscosity sample, with a carbon chain of 10 is affected most by an increase in temperature. This can be seen as an inverse to the previous statement since now, the sample with the higher viscosity caused by the alkyl chain, is now undesirable with a lower viscosity index.

Table 3 shows that increasing the carbon chain length increases the viscosity but here, as temperature is increased this results in a lower viscosity which is undesirable. However, building on this, the two control samples show a large decrease in viscosity as temperature is increased.

To determine viscosity index values, the kinematic viscosity at 40 and 100 °C must be known. To convert to kinematic viscosity, one

must divide the value by the density of the sample. In this work, a fixed density was used, measured at room temperature of 20 °C. Further to this, due to equipment limitations, the highest reliable value for viscosity was 80 °C meaning some data manipulation has been applied whereby taking a logarithm with base 10 of the experimental values and extrapolating the line to 100 °C to acquire this value. The resulting data can be seen in Tables 4 to 6.

Table 4. Conversion of dynamic to kinematic viscosity using measured density at room temperature

Sample	Dynamic viscosity at 20 °C, mPas	Density at 20 °C, g/cm^3	Kinematic viscosity at 20 °C, mm^2/s
1	46	1.489	31
2	84	1.317	64
3	150	1.254	120
Fomblin	463	2.229	208
Leybonol	258	1.063	243

Table 5. Conversion of measured dynamic viscosity to kinematic viscosity at 40 °C using density measured at room temperature

Sample	Measured dynamic viscosity at 40 °C, mPas	Kinematic viscosity at 40 °C, mm^2/s
1	27	18
2	40	30
3	54	43
Fomblin	227	102
Leybonol	131	124

To determine the viscosity index, the following equations are used:

$$VI = \frac{L-U}{L-H}100 \quad \text{if } VI \le 100, \tag{6}$$

$$VI = \frac{10^{(\log H - \log U)/\log Y} - 1}{0.00715} + 100 \quad \text{if } VI > 100, \tag{7}$$

where U is the kinematic viscosity of the test oil at 40 °C and Y is the kinematic viscosity of the test oil at 100 °C.

The L and H values differ depending on the calculation where tabulated values can be found in ISO 2909 and ASTM D2270. For ease of use VI's have been calculated using an online calculator which follows these standards [23], and can be seen in Table 7.

Table 6. Derivation of theoretical kinematic viscosity at 100 °C; adapted from Evans [3], licensed under CC BY-NC 4.0

Sample	Equation of trendline	Theoretical dynamic viscosity at 100 °C, mPas	Theoretical kinematic viscosity at 100 °C, mm^2/s
1	$y = 70.922e^{-0.024x}$	6.434	4.321
2	$y = 110.21e^{-0.026x}$	8.185	6.215
3	$y = 231.18e^{-0.035x}$	6.981	5.566
Fomblin	$y = 985.48e^{-0.039x}$	19.948	8.949
Leybonol	$y = 933.18e^{-0.049x}$	6.953	6.541

Table 7. Calculated viscosity index for all tested samples; adapted from Evans [3], licensed under CC BY-NC 4.0

Sample	Viscosity index	Alkyl chain length
1	138	4
2	151	8
3	80	10
Fomblin	57	n/a
Leybonol	7	n/a

As can be seen in the Table 7, all three of the IL samples have a higher VI than the two control lubricants, suggesting that they are more thermally stable. This is also indirectly backed up by TGA data presented in this work. However, as can be seen in the viscosity vs. temperature graphs (which only went up to 80 °C), the data can be slightly misleading as all of the measured samples have very similar viscosities that are more closely related at 80 °C, but because the control lubricants have a much higher initial viscosity this means their values differ greatly and hence result in a VI value that is lower.

3.5 Contact angle

To gain a deeper understanding of how the lubricants may work in practice, contact angles have been analysed. To form an effective boundary layer in lubrication, the lubricant must 'wet' the surface. Wetting the surface means how the lubricant spreads out and interacts with the surface. There are two methods available for measuring the contact angle, static and dynamic. Static angles are measured when the droplet is standing on the surface and not moving; whereas dynamic angles are measured whilst the liquid droplets is moving (spreading) on the surface, sometimes referred to as advancing or receding angles.

In this work, the dynamic measurement was used to analyse the lubricant's wettability on three key surfaces which were steel, aluminium and Viton. Viton is a brand name that is used as a polymer-type sealant. It is hoped that the three samples will match the control lubricants with values below 90° which would signify good wetting of the surface (Fig. 4); in theory meaning that a good boundary film would be present to prevent friction and wear. Results can be seen in Table 8.

Table 8. Room temperature contact angles measured on aluminium, steel and Viton for all samples; adapted from Evans [3], licensed under CC BY-NC 4.0

Sample	Mean contact angle, °		
	aluminium	steel	Viton
1	64	67	69
2	40	47	61
3	34	24	49
Fomblin	24	29	29
Leybonol	29	24	34

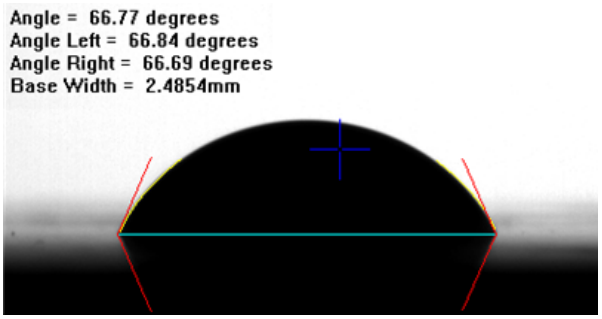

Figure 4. Example contact angle measurement of ionic liquid sample 1 on a steel surface

With regards to the three MIL samples, the data clearly shows another trend relating chemical structure to contact angle. Increasing the length of the carbon chain appears to decrease the contact angle showing better wettability. The values for the three samples are higher on each of the substrates when compared to the control samples however they are all still below 90° and therefore an acceptable value. On the other hand, perhaps the values for the two control lubricants are too low which then results in a boundary film which is too thin which would result in wear when in operation. This hypothesis will be investigated next when analysing lubrication performance in a controlled environment.

3.6 Lubrication studies

In order to assess lubricity and lubricating performance, a coefficient of friction (COF) was acquired. The work was completed using a Bruker UMT TriboLab utilising the high frequency reciprocating rig (HFRR) test, made available through the Henry Royce Institute based at the University of Manchester. Although the graphs produced do not visually conform to a typical Stribeck curve, a lot of information can be obtained. The data can be seen in Figure 5.

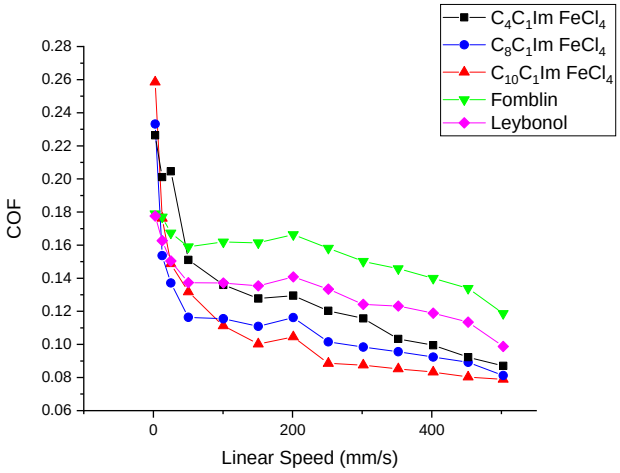

Figure 5. Experimental COF curves based on a high frequency reciprocating rig test at room temperature; adapted from Evans [3], licensed under CC BY-NC 4.0

As expected, the experimental curve shows how the COF varies against speed, which was converted to a linear speed from frequency taking into consideration reciprocating speed and stroke length. Despite an early setting of the lubricants between the ball and reciprocating plate which can be seen, for example by the small fluctuation in COF for $C_4C_1Im\ FeCl_4$, all 5 lines show a minor transition point from what is believed to be boundary lubrication into mixed lubrication at around 200 mm/s in terms of a stereotypical Stribeck curve.

Relating chemical structure to the curves produced, it can be seen a correlation between alkyl chain length and COF, whereby increasing the alkyl chain length appears to decrease the overall COF. A trend that can also be observed when relating viscosity and contact angle, whereby demonstrating the tuneable properties which are so frequently discussed in IL literature.

3.7 X-ray photoelectron spectroscopy (XPS)

Tribochemical reactions are often discussed when analysing ILs as lubricants due to their inherent non-volatility allowing them to be subjected to ultra-high vacuum techniques. Each IL sample was analysed before and after subjection to the lubrication studies. A survey scan was completed to make it possible to spot any new peaks which may arise, as well as high-resolution scans of each element on its own

to investigate how the peak shape changes, if at all, using peak fitting methods that have already been deduced by other authors [24-28].

The survey scans of each IL sample are presented, before and after being subjected to the previously discussed lubrication studies. Survey scans of all samples are shown in Figure 6.

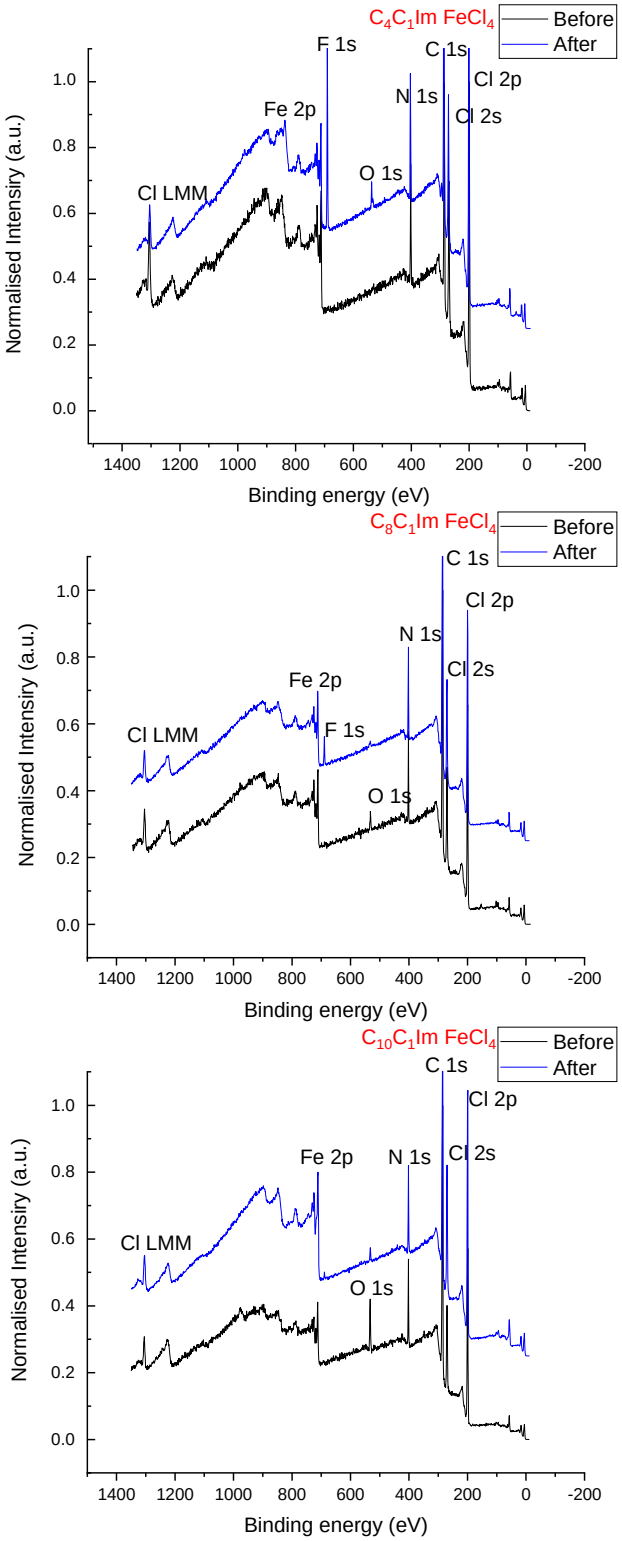

Figure 6. Survey XPS data showing conditions before and after lubrication studies; adapted from Evans [3], licensed under CC BY-NC 4.0

From the survey scans, all expected peaks can be seen in the before scans. There are peaks for carbon 1s at around 284 eV, nitrogen 1s at around 401 eV along with iron and chlorine consisting of multiple peaks. Except for oxygen which is present in spectra

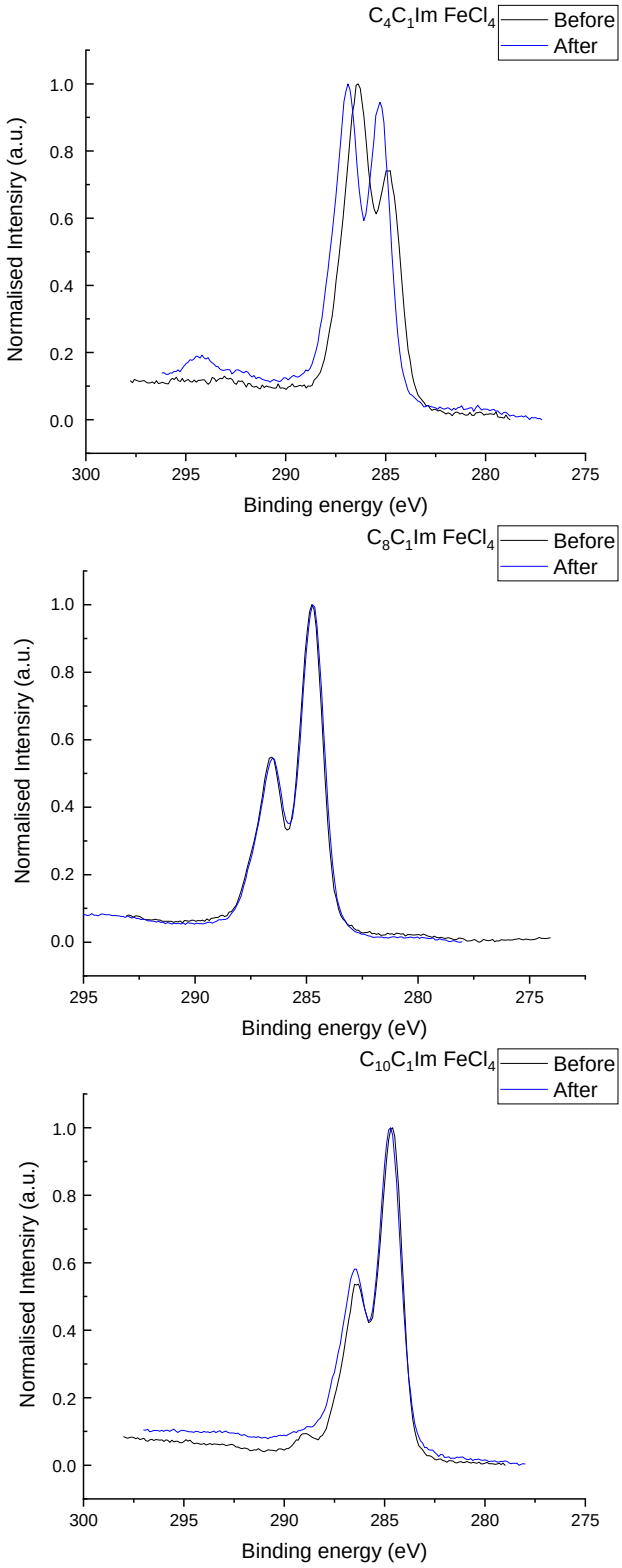

Figure 7. Carbon 1s spectra before and after lubrication studies where the short chain imidazolium cation shows the greatest difference in spectra; adapted from Evans [3], licensed under CC BY-NC 4.0

2 and 3. When analysing the C1s spectra which can be seen in Figure 7, comparing the before and after lubrication studies, there are slight changes in the spectra. The most obvious change appears for the short chain ionic liquid (sample 1). Here, there looks to be an increase in lower binding energy carbon resulting in the two main peaks appearing the same size, though this could also be caused by a decrease in higher binding carbon coming from the imidazolium ring. Further to this, there also appear minor peaks at around 292 – 295 eV for the after lubrication studies. There are no fluorine-containing starting materials in the synthesis (as evidenced by the conditions before lubrication studies) but the control samples were run first which suggests the equipment had not been cleaned properly after these tests had run. Adding to this, it appears that as the machine has progressively been cleaned after each run there is no fluorine present in the latter ionic liquid samples.

4. Conclusion

It has been demonstrated that the three MIL samples show potential to be used as lubricants in a vacuum pump. Data has been presented on magnetism, viscosity, contact angle and lubrication studies, which also includes some XPS analysis of the pre and post lubrication studies samples. Paramagnetism has been demonstrated by all the samples with values that agree with those of the literature. Although not demonstrated in this work, it shows promising results going forward for their potential to be manipulated with a magnetic field for sealant properties whilst also working as a lubricant.

Viscosities and their respective VI's have been presented. Despite showing dynamic viscosity values that are lower than the two control lubricants, their VI's are higher which is deemed advantageous in this field. The operating temperature of the vacuum equipment is believed to be around 85 °C and despite the three MILs showing viscosity values below their commercial counterparts at this temperature, it is also known that the high viscosity of the commercial counterparts can also prove problematic.

Contact angles for the three MIL samples show that they have generally higher angles than their commercial counterparts, but trends can still be seen whereby increasing the alkyl chain length results in a decrease in contact angle. All of the samples show values below 90° which further suggests they will be compatible with the materials found in the vacuum equipment.

The most important data, lubrication studies showed that all of the MIL samples had overall lower COF values suggesting they will perform better as lubricants than current lubricants in use. In addition to this, due to their negligible vapour pressure, they were able to be analysed both before and after lubrication studies. This XPS analysis showed that only the short chained MIL sample had differences in spectra with respect to the C1s. However, as detailed in the text, the extra peaks could be due to contamination whereas the peak shift and change in shape could be due to tribochemical reactions. This then suggests the longer chained MIL samples 2 and 3 may perform well in the vacuum equipment.

This work has then demonstrated that ionic liquids could be used as a lubricant in an elevated-temperature vacuum pump. The ability for the samples, especially samples 2 and 3, to remain unchanged from a chemistry perspective (as demonstrated by XPS) suggests good durability. Early tests also suggest they may be able to act as sealants due to their paramagnetic response to a magnetic field; however, this is yet to be explored and will form the basis of future work whereby studying viscosity and contact angles whilst under a magnetic field.

Acknowledgements

We would like to thank the EPSRC and Edwards Vacuum for their financial support in the project along with the Henry Royce Institute based at the University of Manchester for their equipment in tribological testing.

References

[1] K.J. Anderson, A history of lubricants, MRS Bulletin, Vol. 16, No. 10, 1991, p. 69, DOI: 10.1557/S0883769400055895

[2] The history of synthetic oil (and AMSOIL), available at: https://blog.amsoil.com/the-history-of-synthetic-oil-and-amsoil, accessed: 03.02.2022.

[3] T. Evans, Investigating the Use of Ionic Liquids as a Novel Magnetic Lubricant, PhD thesis, University College London, London, 2023.

[4] C. Ye, W. Liu, Y. Chen, L. Yu, Room-temperature ionic liquids: A novel versatile lubricant, Chemical Communications, Vol. 37, No. 21, 2001, pp. 2244-2245, DOI: 10.1039/b106935g

[5] H. Guo, T.W. Smith, P. Iglesias, The study of hexanoate-based protic ionic liquids used as lubricants in steel-steel contact, Journal of

Molecular Liquids, Vol. 299, 2020, Paper 112208, DOI: 10.1016/j.molliq.2019.112208

[6] R. González, J.L. Viesca, A. Hernández Battez, M. Hadfield, A. Fernández-González, M. Bartolomé, Two phosphonium cation-based ionic liquids as lubricant additive to a polyalphaolefin base oil, Journal of Molecular Liquids, Vol. 293, 2019, Paper 111536, DOI: 10.1016/j.molliq.2019.111536

[7] M. Mahrova, F. Pagano, V. Pejakovic, A. Valea, M. Kalin, A. Igartua, E. Tojo, Pyridinium based dicationic ionic liquids as base lubricants or lubricant additives, Tribology International, Vol. 82, No. A, 2015, pp. 245-254, DOI: 10.1016/j.triboint.2014.10.018

[8] V. Totolin, M. Conte, E. Berriozábal, F. Pagano, I. Minami, N. Dörr, J. Brenner, A. Igartua, Tribological investigations of ionic liquids in ultra-high vacuum environment, Lubrication Science, Vol. 26, No. 7-8, 2014, pp. 514-524, DOI: 10.1002/ls.1224

[9] J. Qu, D.G. Bansal, B. Yu, J.Y. Howe, H. Luo, S. Dai, H. Li, P.J. Blau, B.G. Bunting, G. Mordukhovich, D.J. Smolenski, Antiwear performance and mechanism of an oil-miscible ionic liquid as a lubricant additive, ACS Applied Materials & Interfaces, Vol. 4, No. 2, 2012, pp. 997-1002, DOI: 10.1021/am201646k

[10] C. Gabler, C. Tomastik, J. Brenner, L. Pisarova, N. Doerra, G. Allmaier, Corrosion properties of ammonium based ionic liquids evaluated by SEM-EDX, XPS and ICP-OES, Green Chemistry, Vol. 13, No. 10, 2011, pp. 2869-2877, DOI: 10.1039/c1gc15148g

[11] F.U. Shah, S. Glavatskih, D.R. MacFarlane, A. Somers, M. Forsyth, O.N. Antzutkin, Novel halogen-free chelated orthoborate-phosphonium ionic liquids: Synthesis and tribophysical properties, Physical Chemistry Chemical Physics, Vol. 13, No. 28, 2011, pp. 12865-12873, DOI: 10.1039/c1cp21139k

[12] R. Lu, S. Mori, K. Kobayashi, H. Nanao, Study of tribochemical decomposition of ionic liquids on a nascent steel surface, Applied Surface Science, Vol. 255, No. 22, 2009, pp. 8965-8971, DOI: 10.1016/j.apsusc.2009.03.063

[13] I. Minami, Ionic liquids in tribology, Molecules, Vol. 14, No. 6, 2009, pp. 2286-2305, DOI: 10.3390/molecules14062286

[14] W. Liu, C. Ye, Q. Gong, H. Wang, P. Wang, Tribological performance of room-temperature ionic liquids as lubricant, Tribology Letters, Vol. 13, No. 2, 2002, pp. 81-85, DOI: 10.1023/A:1020148514877

[15] P. Walden, Ueber die molekulargrösse und elektrische leitfähigkeit einiger geschmolzenen salze [About the molecular size and electrical conductivity of some molten salts], Bulletin de l'Académie Impériale des Sciences de St.-Pétersbourg. VI série, Vol. 8, No. 6, 1914, pp. 405-422 [in German].

[16] H.L. Chum, V.R. Koch, L.L. Miller, R.A. Osteryoung, Electrochemical scrutiny of organometallic iron complexes and hexamethylbenzene in a room temperature molten salt, Journal of the American Chemical Society, Vol. 97, No. 11, 1975, pp. 3264-3265, DOI: 10.1021/ja00844a081

[17] C. Nanjundiah, K. Shimizu, R.A. Osteryoung, Electrochemical studies of Fe(II) and Fe(III) in an aluminum chloride-butylpyridinium chloride ionic liquid, Journal of the Electrochemical Society, Vol. 129, No. 11, 1982, pp. 2474-2480, DOI: 10.1149/1.2123587

[18] J.S. Wilkes, J.A. Levisky, R.A. Wilson, C.L. Hussey, Dialkylimidazolium chloroaluminate melts: A new class of room-temperature ionic liquids for electrochemistry, spectroscopy and synthesis, Inorganic Chemistry, Vol. 21, No. 3, 1982, pp. 1263-1264, DOI: 10.1021/ic00133a078

[19] S. Hayashi, H. Hamaguchi, Discovery of a magnetic ionic liquid [bmim]$FeCl_4$, Chemistry Letters, Vol. 33, No. 12, 2004, pp. 1590-1591, DOI: 10.1246/cl.2004.1590

[20] J. Jia, G. Yang, C. Zhang, S. Zhang, Y. Zhang, P. Zhang, Effects of magnetic ionic liquid as a lubricant on the friction and wear behavior of a steel-steel sliding contact under elevated temperatures, Friction, Vol. 9, No. 1, 2021, pp. 61-74, DOI: 10.1007/s40544-019-0324-0

[21] G.A. Bain, J.F. Berry, Diamagnetic corrections and Pascal's constants, Journal of Chemical Education, Vol. 85, No. 4, 2008, pp. 532-536, DOI: 10.1021/ed085p532

[22] K.T. Greeson, N.G. Hall, N.D. Redeker, J.C. Marcischak, L.V. Gilmore, J.A. Boatz, T.C. Le, J.R. Alston, A.J. Guenthner, K.B. Ghiassi, Synthesis and properties of symmetrical *N*,*N*′-bis(alkyl)imidazolium bromotrichloroferrate(III) paramagnetic, room temperature ionic liquids with high short-term thermal stability, Journal of Molecular Liquids, Vol. 265, 2018, pp. 701-710, DOI: 10.1016/j.molliq.2018.06.016

[23] Viscosity index calculator (ISO 2909/ASTM D2270), available at: www.tribonet.org/calculators/viscosity-index-calculator, accessed: 06.06.2022.

[24] A. Zafar, T. Evans, R.G. Palgrave, I. ud-Din, An X-ray photoelectron spectroscopy study of ionic liquids based on a bridged dicationic moiety, Journal of Chemical Research, Vol. 46, No. 2, DOI: 10.1177/17475198221092966

[25] V. Lockett, R. Sedev, C. Bassell, J. Ralston, Angle-resolved X-ray photoelectron spectroscopy of the surface of imidazolium ionic liquids, Physical

Chemistry Chemical Physics, Vol. 10, No. 9, 2008, pp. 1330-1335, DOI: 10.1039/b713584j

[26] T. Yamashita, P. Hayes, Analysis of XPS spectra of Fe^{2+} and Fe^{3+} ions in oxide materials, Applied Surface Science, Vol. 254, No. 8, 2008, pp. 2441-2449, DOI: 10.1016/j.apsusc.2007.09.063

[27] E.F. Smith, F.J.M. Rutten, I.J. Villar-Garcia, D. Briggs, P. Licence, Ionic liquids in vacuo: Analysis of liquid surfaces using ultra-high-vacuum techniques, Langmuir, Vol. 22, No. 22, 2006, pp. 9386-9392, DOI: 10.1021/la061248q

[28] E.F. Smith, I.J. Villar Garcia, D. Briggs, P. Licence, Ionic liquids *in vacuo*; solution-phase X-ray photoelectron spectroscopy, Chemical Communications, Vol. 41, No. 45, 2005, pp. 5633-5635, DOI: 10.1039/b512311a